

A. Chrachri

1       **Effect of FMRFamide on voltage-dependent currents in identified centrifugal**  
2               **neurons of the optic lobe of the cuttlefish, *Sepia officinalis***

3

4    Abdesslam Chrachri

5    University of Plymouth, Dept of Biological Sciences, Drake Circus, Plymouth, PL4

6    8AA, UK and the Marine Biological Association of the UK, Citadel Hill, Plymouth

7    PL1 2PB, UK

8    Phone: 07931150796

9    Email: [aacc@mba.ac.uk](mailto:aacc@mba.ac.uk)

10

11   **Running title:** Membrane currents in centrifugal neurons

12

13   **Key words:** cephalopod, voltage-clamp, potassium current, calcium currents, sodium  
14    current, FMRFamide.

15

16    Summary: FMRFamide modulate the ionic currents in identified centrifugal neurons  
17    in the optic lobe of cuttlefish: thus, FMRFamide could play a key role in visual  
18    processing of these animals.

19

20 **Abstract**

21 Whole-cell patch-clamp recordings from identified centrifugal neurons of the optic  
22 lobe in a slice preparation allowed the characterization of five voltage-dependent  
23 currents; two outward and three inward currents. The outward currents were; the 4-  
24 aminopyridine-sensitive transient potassium or A-current ( $I_A$ ), the TEA-sensitive  
25 sustained current or delayed rectifier ( $I_K$ ). The inward currents were; the tetrodotoxin-  
26 sensitive transient current or sodium current ( $I_{Na}$ ). The second is the cobalt- and  
27 cadmium-sensitive sustained current which is enhanced by barium and blocked by the  
28 dihydropyridine antagonist, nifedipine suggesting that it could be the L-type calcium  
29 current ( $I_{CaL}$ ). Finally, another transient inward current, also carried by calcium, but  
30 unlike the L-type, this current is activated at more negative potentials and resembles  
31 the low-voltage-activated or T-type calcium current ( $I_{CaT}$ ) of other preparations.  
32 Application of the neuropeptide FMRFamide caused a significant attenuation to the  
33 peak amplitude of both sodium and sustained calcium currents without any apparent  
34 effect on the transient calcium current. Furthermore, FMRFamide also caused a  
35 reduction of both outward currents in these centrifugal neurons. The fact that  
36 FMRFamide reduced the magnitude of four of five characterized currents could  
37 suggest that this neuropeptide may act as a strong inhibitory agent on these neurons.  
38

39 **Introduction**

40 Among invertebrates, cephalopods are considered to have an extremely well-  
41 developed eye and a centralized brain (Williamson and Chrachri, 2004), their retina  
42 lacks the vertebrates equivalent of bipolar, amacrine, ganglion cells, etc. and therefore  
43 there is very little visual processing within their retina which instead take place in the  
44 optic lobe. Their retina contains only photoreceptors and supporting cells and it has  
45 been demonstrated that there are some interconnection between the photoreceptors  
46 (Yamamoto et al., 1965; Yamamoto and Takasu, 1984). There is also an extensive  
47 efferent innervation of the retina coming from the inner granular layer of the cortex of  
48 the optic lobe (Young, 1971 and 1974). These efferents are the axons of the  
49 centrifugal neurons that have been demonstrated to be involved in the regulation of  
50 the size of the receptive fields (Tasaki et al., 1982) and the control of the screening  
51 pigment migration (Gleadall et al., 1993). This is still relatively simple compare to the  
52 vertebrate retina.

53 Octopus seem to have a kind of camera eye with an iris and adjustable lens similar to  
54 those of vertebrates, the retina consists of a single layer of photoreceptor cells, and the  
55 optic lobe constitutes the center for visual analysis (Young, 1962). It has also been  
56 suggested that the centrifugal neurons in the optic lobe project towards the  
57 photoreceptors in the retina (Lund, 1979; Saidel, 1979). Although there is little data  
58 about the neuromodulators contained in the centrifugal neurons, the presence of  
59 several neurotransmitters and possible neuromodulators have already been observed in  
60 the optic lobe (Cornwell et al., 1993; Di Cosmo and Di Cristo, 1998; Kito-Yamashita  
61 et al., 1990; Sasayama et al., 1991; Suzuki and Yamamaoto, 2000 and 2002).

62 The neuropeptide FMRFamide (Phe-Met-Arg-Phe-NH<sub>2</sub>) and similar molecules which  
63 are collectively referred to as FMRFa-related peptides (FaRPs) first discovered in  
64 molluscs (Price and Greenberg, 1977 and 1989) are conserved throughout the animal  
65 phyla (Walker et al., 2009). They are abundant in both vertebrate and invertebrate  
66 nervous systems (Espinoza et al., 2000; Dockray et al., 1983; O'Donohue et al., 1984;  
67 Sorenson et al., 1984; Schneider and Taghert, 1988; Greenberg and Price, 1992;  
68 Nelson et al., 1998). In these organisms, FMRFa-like neuropeptide act as  
69 neurotransmitters and neuromodulators. In mammals, FMRFamide induces a variety  
70 of physiological effects, including alterations in blood pressure, respiratory rate,

71 glucose-stimulated insulin release, and behavior (Mues et al., 1982; Sorenson et al.,  
72 1984; Raffa et al., 1986; Thiemermann et al., 1991; Muthal et al., 1997; Nishimura et  
73 al., 2000; Askwith et al., 2000). In cephalopods, it has been demonstrated that FMRFa  
74 is involved in the control of egg laying in *Sepia officinalis* (Henry et al., 1999) as well  
75 as the modulation of L-type calcium currents in heart muscle cells of squid (Chrachri  
76 et al., 2000) and that of both the excitatory and inhibitory postsynaptic currents in  
77 optic lobe neurones of cuttlefish (Chrachri and Williamson, 2003). In 1997, Loi and  
78 Tublitz reported the isolation and characterization of a full-length FaRP cDNA from  
79 the brain of cuttlefish, *Sepia officinalis*. The presence of FMRFa-like  
80 immunoreactivity in the optic lobe of both octopus (Suzuki et al., 2002) and cuttlefish  
81 (Chrachri and Williamson, 2003) has been reported indicating a putative  
82 neurotransmitter or neuromodulator role for this neuropeptide. Furthermore, receptor  
83 binding studies with squid optic lobes have identified G-protein associated FMRFa  
84 binding sites (Chin et al., 1994). Although there have been reports of the ability of this  
85 neuropeptide to modulate the activity of some cephalopod muscles (Loi and Tublitz,  
86 2000; Chrachri et al., 2000) and to potentiate the activity at the squid giant synapse  
87 (Cottrell et al., 1992). However, there is less understanding of its central function  
88 (Chrachri and Williamson, 2003). In metazoans, different FMRFamide-Like Peptides  
89 (FLP) types may exist in the same species, and the same FLP type may occur in  
90 various species (Walker et al. 2009). Recently, a full-length cDNA sequence of an  
91 FMRFamide gene isolated from the cuttlefish, *Sepia pharaonis* was cloned which  
92 shares 93% and 92% similarity with two cuttlefish species, *Sepiella japonica* and  
93 *Sepia officinalis* (Li et al., 2018; Zhu et al., 2020).

94 The mechanisms by which these FaRPs act are not yet fully understood. However, it  
95 has been demonstrated that they either act directly on the membrane conductances of  
96 excitable cells (Cottrell et al., 1984; Colombaioni et al., 1985; Belkin and Abrams,  
97 1993) or through second messenger system (Brezina, 1988; Chiba et al., 1992; Raffa  
98 and Stone, 1996; Chrachri et al., 2000). Furthermore, it has been also shown that  
99 FMRFa can also activate directly one or more types of ligand-gated channels (Cottrell  
100 et al., 1990; Chin et al., 1994; Green et al., 1994).

101 Although the morphology of the centrifugal neurons of the optic lobe of cephalopod  
102 have been studied using both Golgi and cobalt chloride staining (Young, 1974; Saidel,

103 1979), there is no information on the types of ionic currents present in cephalopod  
104 centrifugal neurons. This report provides the first comprehensive study of the voltage-  
105 activated whole-cell membrane currents present in identified centrifugal neurons; we  
106 have characterized five separate ionic currents in these neurons; two outward currents  
107 and three inward currents and studied their modulation by the neuropeptide  
108 FMRFamide.  
109

110 **Material and methods**

111 ***Preparation of slices***

112 Slices were prepared from both male and female cuttlefish, *Sepia officinalis*. Animals  
113 were anaesthetized with 2% ethanol and sacrificed by decapitation. The optic lobe was  
114 rapidly removed and placed in ice-cold  $\text{Ca}^{2+}$ -free artificial sea water (ASW).  
115 Transverse slices of around 300  $\mu\text{m}$  were cut with a vibratome (Campden Instruments,  
116 Loughborough, UK). Slices were kept in a storage chamber in the fridge for up to 1 h  
117 before recording.

118 ***Electrophysiological recordings***

119 Individual slices were transferred to the recording chamber, they were fully  
120 submerged and superfused with oxygenated ASW at a rate of 2-3 ml/min. Centrifugal  
121 neurons were visually identified using an Olympus BX50WI upright microscope with  
122 a x40 water immersion objective lens and equipped with infrared illumination and  
123 video enhanced visualization system consisting of a CCD camera (C7500) and its  
124 controller (C2741-90, Hamamatsu Photonics Ltd., Hertfordshire, UK).

125 Identified centrifugal neurons were studied at room temperature (18-20 °C) with the  
126 whole-cell patch recording techniques (Hamill et al., 1981). Recordings were made  
127 using an Axopatch amplifier (200A, Molecular devices, San Jose, CA 95134, USA)  
128 controlled by PClamp8 software (Molecular devices) for data acquisition, analysis and  
129 storage. Ionic currents were sampled at a rate of 10 kHz and were low-pass filtered at  
130 2 kHz. The pipette series resistance was electronically compensated, as far as possible,  
131 to give voltage errors of only few mV at peak current levels. The capacitance current  
132 response to a  $-10$  mV voltage step, from a holding potential of  $-60$  mV, was recorded  
133 for each neuron and the access resistance calculated. Liquid junction potential was  
134 calculated using the liquid junction calculator provided by the PClamp software. Patch  
135 electrodes with tip resistance of 4.0–6.0 M $\Omega$  were pulled using a horizontal puller  
136 (Sutter Model P-97, Novato, CA, USA) from soda glass capillaries (Intracel, 1.5 mm  
137 o.d., 0.86 mm i.d.). These electrodes were filled with either Aspartate or  $\text{CsCl}_2$  based  
138 internal solution.

139 ***Solution and drugs***

140 The artificial sea water contained (in mM): 430 NaCl; 10 KCl; 10  $\text{CaCl}_2$ ; 30  $\text{MgCl}_2$ ;  
141 25  $\text{MgSO}_4$ ; 0.5  $\text{KH}_2\text{PO}_4$ ; 2.5  $\text{NaHCO}_3$ ; 10 Glucose; 10 HEPES buffer at pH 7.8,

142 osmolarity = 997 mO. Other solutions were made by equimolar substitution of this  
143 basic formula. For example, calcium chloride was replaced with barium chloride to  
144 enhance the inward L-type calcium current. For the calcium free ASW magnesium  
145 was substituted for calcium. Patch pipettes were filled with a solution containing  
146 (mM): 500 Aspartate or CsCl<sub>2</sub>; 10 NaCl; 4 MgCl<sub>2</sub>; 3 EGTA; 20 HEPES, 2 Na<sub>2</sub>ATP,  
147 0.2 Na<sub>3</sub>GTP, 0.2 Lucifer Yellow CH (lithium salt), pH and osmolarity were adjusted  
148 to 7.4 and 870 Osm mol kg<sup>-1</sup> H<sub>2</sub>O with KOH and sucrose, respectively.

149 Pharmacological agents used to block the characterized ionic currents were purchased  
150 from Sigma-Aldrich (Gillingham Dorset, England). These included tetrodotoxin  
151 (TTX), tetraethylammonium chloride (TEA<sup>+</sup>), 4-aminopyridine (4AP), cesium  
152 chloride (CsCl<sub>2</sub>), cobalt chloride (CoCl<sub>2</sub>), barium chloride (BaCl<sub>2</sub>), nifedipine was  
153 dissolved in absolute ethanol to make 5 mM stock solutions and stored at 5 °C in the  
154 dark. Experiments with nifedipine were carried out in dim light to prevent photo-  
155 oxidation. FMRFa was bath applied approximately 10 min after whole cell membrane  
156 seal and break-in.

### 157 ***Statistics***

158 The software package InStat was used for statistical analysis. All data are given as  
159 mean ± SE. Where statistical comparisons are made before and after bath application  
160 of FMRFa, then the two-tailed paired student's *t*-test was employed. If not stated  
161 otherwise, data were denoted as statistically significant when  $P < 0.05$ .

162

163 **Results**

164 The morphology of a typical centrifugal neuron located in the inner granule cell layer  
165 of the optic lobe as revealed by Lucifer yellow staining through the recording  
166 microelectrode is shown in Fig. 1A. These efferent cells have a single axon that  
167 crosses the major neuropil area in the plexiform zone and then exits into one of the  
168 optic nerve bundles. These centrifugal neurons always give off a number of laterally  
169 running branches within the plexiform zone (arrowheads, Fig. 1A) without branching  
170 outside this zone. Their long axon can be seen leaving the slice (Fig. 1A). These cells  
171 can be provisionally identified visually in living slices of the optic lobe based on their  
172 size and position and hence can be readily selected for electrophysiological study and  
173 their identity is further verified from their responses to optic nerve bundle stimulation  
174 which always evoked an antidromic action current and also by dye filling them  
175 through the patch pipette.

176 In cell-attached mode which provides a way not only to record the activity, but also to  
177 stimulate neurons in brain slice preparations. Furthermore, cell-attached recording of  
178 action potential currents is an easy type of recording to do because no breaking of the  
179 patch is involved, and the seal can be loose ( $< 1 \text{ G}\Omega$ ; Kondo and Marty, 1998). Using  
180 this mode of recording action potential current can be evoked by stimulating the  
181 appropriate optic nerve (Fig1. B).

182 Whole-cell patch clamp recordings were obtained from identified centrifugal neurons,  
183 depolarizing pulses of 80 ms duration, from a holding potential of -60 mV, were used  
184 to set the membrane potential at voltages ranging from -60 mV to +60 mV with a 10  
185 mV increments which elicited two main categories of currents; a large outward  
186 current (*open circle*) and an inward current which had an initial large transient  
187 component (*filled circle*) followed by a smaller inward current (*filled triangle*. Fig1.  
188 C). The current-voltage (I-V) curves showing the outward current (*open circles*) and  
189 the fast inward current (*filled circles*, Fig. 1D).

190 ***Whole-cell outward currents***

191 The large outward current observed in these centrifugal neurons at depolarized  
192 potentials was studied using aspartate internal solution in the pipette as well as 1  $\mu\text{M}$   
193 TTX and 2 mM  $\text{CoCl}_2$  in the external solution to block both the sodium and calcium  
194 currents respectively. In this study, we found that in 84% of the centrifugal neurons



195 (21 out of 25) displayed two components of the outward current; a transient fast-  
196 inactivating component and a sustained component (Fig. 2A). In the remaining 16%  
197 (4 neurons), only the sustained component was observed. These two components of  
198 the outward current could be separated using either their voltage or pharmacological  
199 sensitivities (Connor and Stevens, 1971 a, b). If the cell was held at a holding  
200 potential of -40 mV instead of -60 mV, the initial transient component (Fig. 2A)  
201 disappeared during the voltage step protocol (Fig. 2B). Subtracting the outward  
202 currents recorded at -40 mV from those recorded at -60 mV revealed the shape of the  
203 transient or A-current (Fig. 2C). The current-voltage relationships at these two holding  
204 potentials (-40 and -60 mV) as well as the isolated transient or A-current ( $I_A$ ) are  
205 illustrated in Fig. 2D. The addition of 4AP (4 mM) to the bathing solution also  
206 abolished the large transient component of the outward current, leaving only the  
207 sustained outward current (bold trace, Fig. 2E). The current-voltage relationships for  
208 these currents are shown in Fig. 2F. The remaining outward current after either  
209 voltage (Fig. 2B) or pharmacological (Fig. 2E) separation has a sustained time course  
210 and is similar to the delayed rectifier ( $I_K$ ) of other nerve cells. This is confirmed by its  
211 reduction (75%) in the presence of TEA (20 mM, Fig. 2E). These results are  
212 consistent with the presence of two separate outward currents, which from their  
213 kinetics, current-voltage curves, and pharmacological sensitivities, can be  
214 characterized as those already reported outward currents in many preparations,  
215 namely, the delayed rectifier ( $I_K$ ) and the transient A-current ( $I_A$ ).

#### 216 ***Whole-cell inward currents***

217 Inward currents were studied using cesium chloride for the pipette filling solution to  
218 block most of the outward potassium currents we have described above. Under these  
219 conditions, two inward currents were observed in centrifugal neurons of the optic lobe  
220 slice (Fig. 3). The first one had a transient time course (Fig. 3A, star) and the second  
221 had a more sustained time course (Fig. 3A, S). The transient inward current can be  
222 blocked by the addition of TTX (1  $\mu$ M) to the bathing solution, leaving only a  
223 sustained inward current (Fig. 3B). TTX is a known blocker of sodium currents in  
224 many different animal cell types (Hill, 1992). Subtracting current traces after the  
225 application of TTX (Fig. 3B) from those recorded before revealed the TTX-sensitive  
226 current (Fig. 3C). The current-voltage relationships (not shown) of this transient

227 inward current appeared at potentials more positive than -50 mV, peaked at around -  
228 20 mV, and then starts decreasing. Three lines of evidence indicate that this fast  
229 transient inward current is sodium current ( $I_{Na}$ ). Firstly, it was blocked by TTX (Fig.  
230 3B); secondly, it was also blocked in the presence of a sodium-free saline such  
231 replacing sodium with lithium or choline chloride (data not shown); and thirdly, this  
232 inward current could be progressively inactivated by setting the holding potentials at  
233 values more positive than -40 mV. Taken together these data suggest that this current  
234 is probably the sodium current responsible for the rising phase of the action potential  
235 generation.

236 The second inward current had a sustained time course and was not affected either by  
237 TTX (Fig. 3B) or by a sodium-free saline (not shown) and could be increased by the  
238 substituting barium for calcium in the ASW (Fig. 4A). This current could be totally  
239 blocked by the addition of cobalt chloride (2 to 4 mM) to the external solution (Fig.  
240 4B), or cadmium chloride (data not shown) suggesting that it could be carried by  
241 calcium ions. Furthermore, this inward current was more importantly blocked by the  
242 dihydropyridine antagonist, nifedipine, at a concentration of 5  $\mu$ M (Fig. 4C) which  
243 strongly suggest that this current is probably an L-type calcium current ( $I_{Ca,L}$ ). The  
244 current-voltage relationships of this inward calcium current demonstrated that it was  
245 rapidly activated by voltage steps more positive than -40 mV and was maintained  
246 throughout the voltage step with no sign of inactivation. This sustained inward current  
247 achieved a maximum for test steps around 0 or +10 mV and then decreased. In some  
248 of our experiments, a third inward current which was also carried by calcium, but can  
249 be seen only with test pulses from negative holding potential ( $V_h = -80$  mV) had a  
250 transient time course compared to the L-type calcium current (Fig. 4D, trace a). The  
251 current-voltage relationships plot shown in Fig 4E (filled triangles) show that this  
252 current starts to activate at around -50 mV, its amplitude increased progressively with  
253 higher depolarizations, reaching a plateau around -30 mV and then began to decrease.  
254 This current is usually referred to as T-type calcium current ( $I_{Ca,T}$ ) because of its  
255 transient time course. This current is blocked when the holding potential is set at -60  
256 mV or above (Fig. 4D, trace b). This current is similar to the one that have been  
257 reported in heart muscles of squid (Ödblom et al. 2000). In these centrifugal neurons,  
258 the L-type calcium was encountered invariably. By contrast, the T-type calcium

259 currents were rare and we have only seen them in 5 centrifugal neurons. This transient  
260 inward current had similar pharmacological characteristics to that of reported in heart  
261 muscle cells of squid (Ödblom et al., 2000; Chrachri et al., 2000), in that it was only  
262 partially blocked by 2-5  $\mu\text{M}$  nifedipine. This dihydropyridine antagonist has been  
263 shown to block preferentially the L-type calcium current in many preparations (Fox et  
264 al., 1987; Wang et al., 1996; Chrachri and Williamson, 1997). However, as for the  
265 isolated heart muscle cells, nifedipine also blocks the transient calcium current by  
266 about 48.4% ( $n = 3$ ).

### 267 ***Effect of FMRFa on the outward current***

268 To investigate the effect of the neuropeptide FMRFa on the outward potassium  
269 currents in the centrifugal neurons, we bath applied FMRFa (1  $\mu\text{M}$ ) to voltage  
270 clamped centrifugal neurons and found that this neuropeptide induced a significant  
271 reduction of the overall potassium current in 11 out of 15 centrifugal neurons. At a  
272 holding potential of -60 mV, the reduction of the potassium currents was significant ( $p$   
273  $< 0.0001$ ) and was about  $39.83 \pm 7.92\%$  ( $n = 11$ ). When the holding potential was set  
274 to -40 mV and therefore to study the effect of FMRFa on the delayed rectifier ( $I_k$ ) on  
275 its own, the reduction of  $I_k$  by FMRFa was also reduced significantly ( $p = 0.0028$ ) by  
276 about  $31.27 \pm 10.45\%$  ( $n = 5$ ). A typical experiment demonstrating the FMRFa-  
277 induced reduction of the peak current of both the fast-inactivating and sustained  
278 potassium currents is illustrated in Fig. 5. The effect of FMRFa on these two  
279 components of the potassium currents was reversible (Fig. 5C). Subtracting the  
280 current traces in the presence of FMRFa (Fig. 5B) from the control current traces (Fig.  
281 5A) revealed the FMRFa-sensitive potassium currents (Fig. 5D). In the remaining 4  
282 centrifugal neurons, FMRFa did not appear to have any apparent effect on both  
283 components of the outward potassium current (data not shown).

### 284 ***FMRFa-mediated attenuation of the inward sodium current ( $I_{Na}$ )***

285 Bath application of FMRFa (1  $\mu\text{M}$ ) seems to induce a reduction in the magnitude of  
286 this inward sodium current. Fig. 6A illustrates a typical example, 5 minutes after bath  
287 application of FMRFa the amplitude of the sodium current was reduced by about  
288 28.8% (Fig. 6A, grey line). 8 minutes after the addition of FMRFa, the amplitude of  
289  $I_{Na}$  was reduced even further, this time by about 44.44% (Fig. 6A, thick line). The  
290 effect of FMRFa on the  $I_{Na}$  is also illustrated in Fig. 6B, where the current-voltage

291 relationship demonstrates that FMRFa reduces  $I_{Na}$  over most of the voltage ranges.  
292 Pooled data from 3 experiments demonstrated that FMRFa induced a significant ( $p =$   
293  $0.01$ ) decrease of the sodium current by about  $41.74 \pm 5.94\%$ .

294 ***Effect of FMRFa on L-type and T-type calcium currents***

295 Fig. 6, not only demonstrates that FMRFa reduced the peak amplitude of the  $I_{Na}$  (star),  
296 but also decreased that of the sustained L-type calcium current (triangle). Unlike in the  
297 case of potassium currents, bath application of FMRFa ( $1 \mu\text{M}$ ) always resulted in  
298 reducing the calcium current. The magnitude of the peak  $I_{Ca,L}$  was reduced  
299 significantly ( $p = 0.0002$ ) by about  $64.92 \pm 5\%$  ( $n = 8$ ). An example is illustrated in  
300 Fig. 7A (right panel), where the inhibition of  $I_{Ca,L}$  was about 52%. The current-voltage  
301 curves show that FMRFa reduction of the amplitude of  $I_{Ca,L}$  is over most of the  
302 voltage ranges. However, the reduction induced by FMRFa decreased for steps to  
303 depolarized voltages more positive than +10 mV (Fig. 7B). This figure also  
304 demonstrates that FMRFa ( $1 \mu\text{M}$ ) didn't have any noticeable effect on the T-type  
305 calcium current (Fig. 7A, left panel). The current/voltage plot provides further  
306 evidence that FMRFa selectively affects the amplitude of  $I_{Ca,L}$ , but not the  $I_{Ca,T}$  (grey  
307 circles, Fig. 7B). Figure 8 illustrates the time course of the onset of the inhibition of  
308  $I_{Ca,L}$  by FMRFamide and the subsequent recovery by washing, and demonstrates that  
309 the inhibition was relatively rapid and fully reversible.

310

311 **Discussion**

312 This study has characterized the electrical properties in identified centrifugal neurons  
313 in the optic lobe slice preparation of the cuttlefish, *Sepia officinalis*, using whole-cell  
314 patch clamp we documented the presence of five voltage-sensitive ionic currents and  
315 studied their modulation by the neuropeptide FMRFa. These voltage-activated  
316 currents comprised; tree inward currents; one carried by sodium ( $I_{Na}$ ) and the two  
317 others by calcium ( $I_{CaL}$  and  $I_{CaT}$ ), and two outward currents that were selective for  
318 potassium ( $I_A$ ,  $I_K$ ). The effect of the neuropeptide, FMRFa, on these currents is also  
319 discussed.

320 *Na<sup>+</sup> current*

321 The rapid inward current is activated immediately after the onset of the command  
322 pulse, reaches a peak in few milliseconds, and inactivated within 10 ms. As in many  
323 other excitable tissues (Lo and Shrager, 1981; Neher, 1971; Lasater, 1986), this fast  
324 inward current is carried by sodium, in that it is blocked when the optic lobe slice is  
325 perfused with a sodium-free ASW, it is also totally blocked by TTX (1 $\mu$ M) and is  
326 inactivated when the cells is held at values more positive than -40 mV. This  $I_{Na}$  was  
327 present in all of the centrifugal neurons we have recorded from (without exception).  
328 The presence of such sodium current in these centrifugal neurons was not surprising  
329 because these neurons send their axons a long distance towards the retina (Saidel,  
330 1979) and therefore it is possible that these centrifugal neurons will need action  
331 potentials to carry their information towards the photoreceptors located in the retina.  
332 Whole-cell patch clamp recordings from other cell types within the optic lobe (i.e.  
333 medulla and amacrine) demonstrated that these neurons do not extend their axons  
334 towards the retina, and that only a few of them displayed sodium currents it is present  
335 in only about a third of them (Chrachri and Williamson, unpublished data).

336 *Ca<sup>2+</sup> currents*

337 A vast amount of investigations have been carried out on the voltage-dependent  
338 calcium currents in a variety of neuron and muscle cells (Liu and Lasater, 1994;  
339 Ödblom et al., 2000). In the present investigation we have identified two more inward  
340 currents, one of which have a sustained time course and the other have a transient time  
341 course. Both of them were carried by calcium ions (Fig. 4). On the basis of its  
342 kinetics, ion specificity and pharmacological sensitivity, the sustained inward current

343 resembles to the high voltage-activated calcium (HVA), or L-type calcium current  
344 reported in a variety of other cell types (Carbone and Lux 1984,; Fox et al., 1987). The  
345 other voltage-dependent calcium current is similar to the transient, low-threshold  
346 (LVA) or T-type (Nowycky et al., 1985) which only appeared when neurons were held  
347 at potentials more negative than -60 mV. This current had similar kinetics and  
348 pharmacological characteristics to that reported in squid isolated heart muscle cells  
349 (Ödholm et al., 2000; Chrachri et al., 2000), in that it showed higher selectivity to  
350 blockade by nickel chloride than the L-type calcium current (data not shown) which is  
351 similar to reports in other preparations (Mitra and Morad, 1986; Hagiwara et al., 1988;  
352 Wu and Lipsius, 1990). It was also partially blocked by nifedipine which has been  
353 shown to have a more specific effect on the L-type calcium current (Scott et al., 1991),  
354 but similar results have been reported in atrial cells (Bean, 1985), retinal ganglion  
355 cells (Liu and Lasater, 1994) and olfactory bulb neurons (Wang et al., 1996).

#### 356 *K<sup>+</sup> currents*

357 Under voltage-clamp conditions, when centrifugal neurons were depolarized to  
358 voltages more positive than -30 mV from a holding potential of -60 mV, two outward  
359 potassium currents were detected, the delayed rectifier or  $I_K$  and the A-current or  $I_A$ .  
360 These two time- and voltage-dependent  $K^+$  currents were distinguishable both by their  
361 pharmacological sensitivity to 4AP, and by their voltage-dependent inactivation  
362 (Connor and Stevens, 1971 a, b; Thompson, 1977). Similar results have been reported  
363 in other cephalopod cells (Llano and Bookmanm, 1986; Lucero et al., 1992; Chrachri  
364 and Williamson, 1997). TEA at a concentration of 20 mmol l<sup>-1</sup> blocked most of the  
365 delayed rectifier  $K^+$  currents in centrifugal neurons. These concentrations of TEA are  
366 relatively very low compared to those needed to block the similar  $I_K$  in sensory hair  
367 cells of the squid statocysts (Chrachri and Williamson, 1997), the squid giant axons  
368 (Tasaki and Hagiwara, 1957) and isolated heart muscle cells (Ödholm et al., 2000)  
369 where very high concentrations of TEA were needed. The delayed rectifier activates at  
370 potentials more positive than does the A-type current and show no appreciable  
371 inactivation during a depolarizing voltage step also contribute to action potential  
372 repolarization (Saito and Wu, 1991). The effects of blockade of delayed rectifier in  
373 centrifugal neurons by TEA are consistent with the pharmacology of other delayed-  
374 rectifier subtypes of  $K^+$  channels (see Hille, 1992).

375 *FMRFa-mediated effect on the centrifugal neurons of the optic lobe*

376 We have demonstrated that the neuropeptide, FMRFa, significantly reduced the  
377 inward  $\text{Na}^+$  current in the centrifugal neurons of the optic lobe, the effect was voltage  
378 dependent, it lasts as long as the peptide is present and finally the reduction of  $\text{Na}^+$   
379 current by FMRFa is partially reversible. Furthermore, This FMRFa-induced  
380 inhibition was also seen as a reduction of the antidromic action current following  
381 stimulation of the appropriate optic nerve bundle (not shown). Modulation of  $\text{Na}^+$   
382 current is likely to be important in the regulation of the centrifugal neuron's  
383 excitability. The reduction of the  $I_{\text{Na}}$  by FMRFa will increase the threshold of the  
384 action potential and so contribute to the inhibitory effects of FMRFa on the  
385 excitability of the cell, possibly resulting in suppressing on-going firing activity as  
386 well as preventing the generation of new discharges. Inhibition of this current by  
387 FMRFa has been shown in other molluscan preparations, the peptidergic caudo-dorsal  
388 cells of the mollusc *Lymnaea stagnalis* (Brussaard et al., 1991).

389 Another action of FMRFa is to attenuate the voltage-dependent sustained calcium  
390 current. Attenuation of this type of calcium current by FMRFa has also been described  
391 in a number of other types of cells (Kramer et al., 1988; Man-Song-Hing et al., 1989;  
392 Yakel, 1991; Chrachri et al., 2000). However, this neuropeptide didn't have any effect  
393 on the T-type calcium current. Similar selectivity for the FMRFamide-induced  
394 reduction of the calcium current has been reported in neurons of *Aplysia californica*  
395 (Brezina et al., 1987), in isolated heart muscle cells of squid (Chrachri et al., 2000). It  
396 is probably not surprising that FMRFa affected  $I_{\text{Ca,L}}$  but not  $I_{\text{Ca,T}}$  in centrifugal  
397 neurons. It has been reported that this neuropeptide reduced the amplitude of  
398 spontaneous excitatory postsynaptic currents (sEPSCs) in centrifugal neurons.  
399 However, when these sEPSCs occurred in bursting mode, FMRFa did change the  
400 amplitude of sEPSCs without any significant modulation of the frequency their  
401 rhythmic activity (Chrachri unpublished data). This transient current has been  
402 proposed to control rhythmic membrane oscillations central neurons (Llinas and  
403 Yarom, 1981) and therefore the lack of effect of FMRFa on  $I_{\text{Ca,T}}$  might have been  
404 expected.



405 We have also presented evidence that application of FMRFa evoked a partial blockade  
406 of both characterized outward; the  $I_A$  as well as the  $I_{kv}$  currents in these  
407 morphologically identifiable centrifugal neurons of the optic lobe.

408 *Physiological relevance of the action of FMRFa*

409 The reduction of the amplitude of the L-type calcium current in the centrifugal  
410 neurons would be a relevant physiological action for FMRFa.  $Ca^{2+}$  channels in  
411 neurons are frequent targets of neurotransmitter modulation, with suppression or  
412 enhancement of  $Ca^{2+}$  channel activity being a common outcome, albeit *via* different  
413 mechanisms (Gerschenfeld et al., 1989; Yakel, 1991). The fact that this neuropeptide  
414 affect the ionic currents (this study) and the postsynaptic currents of these efferent  
415 neurons (Chrachri and Williamson, 2003) would undoubtedly suggest a role for the  
416 retinal cells which are under the control of these centrifugal neurons (Saidel, 1979).  
417 There is a wide distribution of FMRFa like immunoreactivity in the optic lobe of  
418 cephalopods (Suzuki et al., 2002; Chrachri and Williamson, 2003). Thus the FMRFa-  
419 induced effects on the centrifugal neurons we have reported in this paper may  
420 probably mirror the endogenous modulation of the centrifugal neuron by  
421 FMRFamidergic nerve fibres. Using behavioral studies it has been demonstrated that  
422 the optic lobe of *sepia officinalis* may provides a system for coding, sorting and  
423 decoding the visual input to produce a relevant behaviour (Chichery and Chanelet,  
424 1976). The fact that the application of FMRFa induced not only a modulation of ionic  
425 currents (this report), but also appears to act presynaptically to modulate both  
426 spontaneous excitatory and inhibitory currents in the same preparation (Chrachri and  
427 Williamson, 2003) could suggest that this neuropeptide may play a crucial role in  
428 visual processing. Similar roles for FMRFa in visual processing have been described  
429 in the locust optic lobe (Rémy et al., 1988) and in fish (Wang et al., 2000).

430

431

432



433 **List of symbols and abbreviations**

434 o.gr.: outer granule cell layer; i.gr.: inner granule cell layer; pl: plexiform zone; 4AP:  
435 4-aminopyridine; TEA: tetra-ethyl ammonium; TTX: tetrodotoxin

436 **Competing interests**

437 I declare that there are no competing or financial interests.

438 **Funding**

439 This work was supported by the Wellcome Trust.

440

441 **References**

- 442 **Askwith, C. C., Cheng, C., Ikuma, M., Benson, C. and Welsh, M. J.** (2000).  
443 Neuropeptide FF and FMRFamide potentiate acid-evoked currents from sensory  
444 neurons and proton-gated DEG/ENaC channels. *Neuron* **26**, 133-141. doi:  
445 [10.1016/s0896-6273\(00\)81144-7](https://doi.org/10.1016/s0896-6273(00)81144-7)
- 446 **Bean, B. P.** (1985). 2 kinds of calcium channels in canine atrial cells- differences in  
447 kinetics, selectivity and pharmacology. *J. Gen. Physiol.* **86(1)**, 1-30. doi:  
448 [10.1085/jgp.86.1.1](https://doi.org/10.1085/jgp.86.1.1)
- 449 **Belkin, K. J. and Abrams, T. W.** (1993). FMRFamide produces biphasic modulation  
450 of the LFS motor-neurons in the neural circuit of the siphon withdrawal reflex of  
451 *Aplysia* by activating Na<sup>+</sup> and K<sup>+</sup> currents. *J. Neurosci.* **13**, 5139-5152  
452 doi.org/10.1523/JNEUROSCI.13-12-05139.1993
- 453 **Brezina, V., Eckert, R. and Erxleben, C.** (1987). Suppression of calcium current by  
454 endogenous neuropeptide in neurones of *Aplysia californica*. *J. Physiol. (Lond)* **388**,  
455 565-595. doi: [10.1113/jphysiol.1987.sp016632](https://doi.org/10.1113/jphysiol.1987.sp016632)
- 456 **Brezina, V.** (1988). Guanosine 5'-triphosphate analog activates potassium current  
457 modulated by neurotransmitters in *Aplysia* neurons. *J. Physiol. (Lond)* **407**, 15-40.  
458 doi.org/10.1113/jphysiol.1988.sp017401
- 459 **Brussaard, A.B., Lodder, J. C., Termaat, A., Devlieger, T. A. and, Kits, K. S.**  
460 (1991). Inhibitory modulation by FMRFamide of the voltage-gated sodium current in  
461 identified neurons in *Lymnaea stagnalis*. *J. Physiol. (Lond)* **441**, 385-404. doi:  
462 [10.1113/jphysiol.1991.sp018757](https://doi.org/10.1113/jphysiol.1991.sp018757)
- 463 **Carbone, E. and Lux, H. D.** (1984). A low voltage-activated fully inactivating Ca  
464 channel in vertebrate sensory neurones. *Nature (Lond)* **310**, 501-502. doi:  
465 [10.1038/310501a0](https://doi.org/10.1038/310501a0)
- 466 **Chiba, O., Sasaki, K., Higuchi, H. and Takashima, K.** (1992). G-protein mediating  
467 the slow depolarization induced by FMRFamide in the ganglion cells of *Aplysia*.  
468 *Neurosci. Res.* **15**, 255-264. doi: [10.1016/0168-0102\(92\)90046-f](https://doi.org/10.1016/0168-0102(92)90046-f)
- 469 **Chin, G. J., Payza, K., Price, D. A., Greenberg, M. J. and Doble, K. E.** (1994)  
470 Characterization and solubilization of the FMRFamide receptor of squid. *Biol. Bull.*  
471 **187**, 185-199. doi: [10.2307/1542241](https://doi.org/10.2307/1542241)

- 472 **Chichery, R. and Chanelet, J.** (1976). Motor and behavioral responses obtained by  
473 stimulation with chronic electrodes of the optic lobe of *Sepia officinalis*. *Brain Res.*  
474 **105**, 525-32. [doi.org/10.1016/0006-8993\(76\)90598-9](https://doi.org/10.1016/0006-8993(76)90598-9)
- 475 **Chrachri, A. and Williamson, R.** (1997). Voltage-dependent conductances in  
476 cephalopod primary sensory hair cells. *J. Neurophysiol.* **78**, 3125-3132.  
477 [doi.org/10.1152/jn.1997.78.6.3125](https://doi.org/10.1152/jn.1997.78.6.3125)
- 478 **Chrachri, A., Ödöblom, M. and Williamson, R.** (2000). G protein-mediated  
479 FMRFamideergic modulation of calcium influx in dissociated heart muscle cells from  
480 squid, *Loligo forbesii*. *J. Physiol. (Lond)* **525** (2), 471-482. [doi: 10.1111/j.1469-](https://doi.org/10.1111/j.1469-7793.2000.00471.x)  
481 [7793.2000.00471.x](https://doi.org/10.1111/j.1469-7793.2000.00471.x)
- 482 **Chrachri, A. and Williamson, R.** (2003). Modulation of spontaneous and evoked  
483 EPSCs and IPSCs in optic lobe neurons of cuttlefish, *Sepia officinalis* by the  
484 neuropeptide FMRF-amide. *Eur. J. Neurosci.* **17** (3), 526-536.  
485 [doi.org/10.1046/j.1460-9568.2003.02478.x](https://doi.org/10.1046/j.1460-9568.2003.02478.x)
- 486 **Colombaioni, L., Paupardin-Tritsch, D., Vidal, P. P. and Gerschenfeld, H. M.**  
487 (1985). The neuropeptide FMRF-amide decreases both the Ca<sup>2+</sup> conductance and a  
488 cyclic 3',5'-adenosine monophosphate-dependent K<sup>+</sup> conductance in identified  
489 molluscan neurones. *J. Neurosci.* **5**, 2533-2538. [doi.org/10.1523/JNEUROSCI.05-09-](https://doi.org/10.1523/JNEUROSCI.05-09-02533)  
490 [02533](https://doi.org/10.1523/JNEUROSCI.05-09-02533)
- 491 **Connor, J. A. and Stevens, C. F.** (1971a). Inward and delayed outward membrane  
492 currents in isolated neural somata under voltage-clamp. *J. Physiol. (Lond)* **213**:1-19.  
493 [doi.org/10.1113/jphysiol](https://doi.org/10.1113/jphysiol)
- 494 **Connor, J. A. and Stevens, C. F.** (1971b) Voltage-clamp studies of a transient  
495 outward current in a gastropod neural somata. *J. Physiol. (Lond)* **213**, 21-30. [doi:](https://doi.org/10.1113/jphysiol.1971.sp009365)  
496 [10.1113/jphysiol.1971.sp009365](https://doi.org/10.1113/jphysiol.1971.sp009365)
- 497 **Cornwell, C.J., Messenger, J.B. and Williamson, R.** (1993). Distribution of GABA-  
498 like immunoreactivity in the octopus brain, *Brain Res.* **621**, 353-357.  
499 [doi.org/10.1016/0006-8993\(93\)90127-9](https://doi.org/10.1016/0006-8993(93)90127-9)
- 500 **Cottrell, G. A., Davies, N. W. and Green, K. A.** (1984). Multiple actions of a  
501 molluscan cardioexcitatory neuropeptide and related peptides on identified *Helix*  
502 neurones. *J. Physiol. (Lond)* **356**, 315-333. [doi.org/10.1113/jphysiol](https://doi.org/10.1113/jphysiol)

- 503 **Cottrell, G. A., Green, K. A. and Davies, N. W.** (1990). The neuropeptide  
504 FMRFamide can activate a ligand-gated ion channel in *Helix* neurones. *Pflügers Arch.*  
505 **416**, 612-614. doi: [10.1007/BF00382698](https://doi.org/10.1007/BF00382698)
- 506 **Cottrell, G. A., Lin, J. W., Llinas, R., Price, D. A., Sugimori, M. and Stanley, E.**  
507 **F.** (1992). FMRF-amide-related peptides potentiate transmission at the squid giant  
508 synapse. *Exp. Physiol.* **77**, 881-889. doi.org/[10.1113/expphysiol](https://doi.org/10.1113/expphysiol)
- 509 **Di Cosmo, A. and Di Cristo, C.** (1998). Neuropeptidergic control of the optic gland  
510 of *Octopus vulgaris*: FMRF-amide and GnRH immunoreactivity, *J. Comp. Neurol.*  
511 **398**, 1-12. doi: [10.1002/\(sici\)1096-9861\(19980817\)398:1<1::aid-cne1>3.0.co;2-5](https://doi.org/10.1002/(sici)1096-9861(19980817)398:1<1::aid-cne1>3.0.co;2-5)
- 512 **Dockray, G. J., Reeve, J. R., Shively, J., Gayton, R. J. and Barnard, C. S. A.**  
513 (1983) Novel active peptide from chicken brain identified by antibodies to  
514 FMRFamide. *Nature* **305**: 328-330. doi: [10.1038/305328a0](https://doi.org/10.1038/305328a0)
- 515 **Espinoza, E., Carrigan, M., Thomas, S.G., Shaw, G. and Edison, A.S.** (2000). A  
516 statistical view of FMRFamide neuropeptide diversity. *Mol. Neurobiol.* **21**, 35–56.  
517 doi: [10.1385/MN:21:1-2:035](https://doi.org/10.1385/MN:21:1-2:035)
- 518 **Fox, A. P., Nowycky, M. C. and Tsien, R. W.** (1987). Kinetic and pharmacological  
519 properties distinguishing three types of calcium currents in chick sensory neurones. *J.*  
520 *Physiol. (Lond)* **394**, 149-172. doi: [10.1113/jphysiol.1987.sp016864](https://doi.org/10.1113/jphysiol.1987.sp016864)
- 521 **Gerschenfeld, H. M., Paupardin-Tritsch, D., Hammond, C. and Harris-Warrick,**  
522 **R.** (1989) Intracellular mechanism of neurotransmitter-induced modulations of  
523 voltage-dependent Ca<sup>2+</sup> current in snail neurons. *Cell. Biol. Int. Rep.* **13 (12)**, 1141-  
524 1154. doi.org/[10.1016/0309-1651\(89\)90028-3](https://doi.org/10.1016/0309-1651(89)90028-3)
- 525 **Gleadall, I. G., Ohtsu, K., Gleadall, E. and Tsukahara, Y.** (1993). Screening-  
526 pigment migration in the *Octopus* retina includes control by dopaminergic efferents. *J.*  
527 *Exp. Biol.* **185**, 1-16. . <http://jeb.biologists.org/content/185/1/1>
- 528 **Green, K. A., Falconer, S. W. and Cottrell, G. A.** (1994). The neuropeptide Phe-  
529 Met-Arg-Phe-NH<sub>2</sub> (FMRFamide) directly gates two ion channels in an identified  
530 *Helix* neurone. *Pflügers Arch.* **428**, 232-240. doi: [10.1007/BF00724502](https://doi.org/10.1007/BF00724502)
- 531 **Greenberg, M. J. and Price, D. A.** (1992). Relationships among the FMRFamide-  
532 like peptides. *Prog. Brain Res.* **92**, 25-37. doi: [10.1016/s0079-6123\(08\)61162-0](https://doi.org/10.1016/s0079-6123(08)61162-0)

- 533 **Hagiwara, N., Irishawa, H. and Kameyama, M.** (1988). Contribution to two types  
534 of calcium currents to pacemaker potentials of rabbit sinoatrial node cell. *J. Physiol.*  
535 (*Lond*) **395**, 233-253. <https://doi.org/10.1113/jphysiol>
- 536 **Hamill, O. P., Marty, A., Neher, E., Sackmann, B. and Sigworth, F. J.** (1981).  
537 Improved patch-clamp and cell-free membrane patches. *Pflügers Arch* **391**:91-100.  
538 [doi: 10.1007/BF00656997](https://doi.org/10.1007/BF00656997)
- 539 Henry J, Zatylny C Boucaud-Camou E (1999) Peptidergic control of egg-laying in the  
540 cephalopod *Sepia officinalis*: involvement of FMRFamide and FMRFamide-related  
541 peptides. *Peptides* **20(9)**, 106-1070. [doi: 10.1016/s0196-9781\(99\)00102-3](https://doi.org/10.1016/s0196-9781(99)00102-3)
- 542 **Hille, B.** (1992). Ionic channels of excitable membranes. Sinauer, Sunderland, MA.,  
543 **Kito-Yamashita, T., Haga, C., Hirai, K., Uemura, T., Kondo, H. and Kosaka, K.**  
544 (1990). Localization of serotonin immunoreactivity in cephalopod visual system,  
545 *Brain Res.* **521**, 81–88. [doi: 10.1016/0006-8993\(90\)91527-n](https://doi.org/10.1016/0006-8993(90)91527-n)
- 546 **Kondo, S. and Marty, A.** (1998). Synaptic currents at individual connections among  
547 stellate cells in rat cerebellar slices. *J. Physiol.* **509**, 221-232  
548 <https://doi.org/10.1111/j.1469-7793.1998.233bo.x>
- 549 **Kramer, R., Levitan E., Carrow G. and Levitan I.** (1988). Modulation of a  
550 subthreshold calcium current by the neuropeptide FMRFamide in *Aplysia* neuron. *J.*  
551 *Neurophysiol.* **60**, 1728-1738. [doi.org/10.1152/jn.1988.60.5.1728](https://doi.org/10.1152/jn.1988.60.5.1728)
- 552 **Lasater, E. M.** (1986). Ionic currents of cultured horizontal cells isolated from white  
553 perch retina. *J. Neurophysiol.* **55**, 499-513. [doi.org/10.1152/jn.1986.55.3.499](https://doi.org/10.1152/jn.1986.55.3.499)
- 554 **Li, Y., Cao, Z., Li, H., Liu, H., Lü, Z. and Chi, C.** (2018). Identification,  
555 Characterization, and Expression Analysis of a FMRFamide-Like Peptide Gene in the  
556 Common Chinese Cuttlefish (*Sepiella japonica*). *Molecules* **23**, 742;  
557 [doi:10.3390/molecules23040742](https://doi.org/10.3390/molecules23040742)
- 558 **Liu, Y. and Lasater, E. M.** (1994). Calcium currents in turtle retinal ganglion cells. I.  
559 The properties of T- and L-type currents. *J. Neurophysiol.* **71**, 733-742.  
560 [doi.org/10.1152/jn.1994.71.2.733](https://doi.org/10.1152/jn.1994.71.2.733)
- 561 **Llano, I. and Bookman, R. J.** (1986). Ionic conductances of squid giant fiber lobe  
562 neurons. *J. Gen. Physiol.* **88**, 543-569. [doi: 10.1085/jgp.88.4.543](https://doi.org/10.1085/jgp.88.4.543)

- 563 **Llinas, R. and Yarom, Y.** (1981). Properties and distribution of ionic conductances  
564 generating electroresponsiveness of mammalian inferior olivary neurons *in vitro*. *J.*  
565 *Physiol. (Lond)* **315**, 569-584. <https://doi.org/10.1113/jphysiol.1981.sp013764>
- 566 **Lo, M. V. C. and Shrager, P.** (1981). Block and inactivation of sodium channels in  
567 nerve by amino acid derivatives. *Biophys. J.* **35**, 31-43. [doi.org/10.1016/0165-](https://doi.org/10.1016/0165-0270(93)90069-4)  
568 [0270\(93\)90069-4](https://doi.org/10.1016/0165-0270(93)90069-4)
- 569 **Loi, P. K. and Tublitz, N. J.** (1997). Molecular analysis of FMRFamide- and  
570 FMRFamide-related peptides (FaRPs) in the cuttlefish, *Sepia officinalis*. *J. Exp. Biol.*  
571 **200**, 1483-1489.
- 572 **Loi, P. K. and Tublitz, N. J.** (2000). Role of glutamate and FMRFamide-related  
573 peptides at the chromatophore neuromuscular junction in the cuttlefish, *Sepia*  
574 *officinalis*. *J. Comp. Neurol.* **420**, 499-511. doi: [10.1002/\(SICI\)1096-](https://doi.org/10.1002/(SICI)1096-9861(20000515)420:4<499::AID-CNE7>3.0.CO;2-E)  
575 [9861\(20000515\)420:4<499::AID-CNE7>3.0.CO;2-E](https://doi.org/10.1002/(SICI)1096-9861(20000515)420:4<499::AID-CNE7>3.0.CO;2-E)
- 576 **Lucero, M. T. Horrigan, F. T. and Gilly, V. F.** (1992). Electrical responses to  
577 chemical stimulation of squid olfactory receptor cells. *J. Exp. Biol.* **162**, 231-249.  
578 doi: [10.1098/rstb.2000.0670](https://doi.org/10.1098/rstb.2000.0670)
- 579 **Mitra, R. and Morad, M.** (1986). Two types of calcium channel in guinea pig  
580 ventricular myocytes. *Proc. Natl. Acad. Sci. USA* **83**, 5340-5344. doi:  
581 [10.1073/pnas.83.14.5340](https://doi.org/10.1073/pnas.83.14.5340)
- 582 **Mues, G., Fuchs, I., Wei, E. T., Weber, E., Evans, C. J., Barchas, J. D. and**  
583 **Chang, J. K.** (1982). Blood pressure elevation in rats by peripheral administration of  
584 Tyr-Gly-Gly-Phe-Met-Arg-Phe and the invertebrate neuropeptide, Phe-Met-Arg-Phe-  
585 NH<sub>2</sub>. *Life Sciences* **31**, 2555-2561. doi: [10.1016/0024-3205\(82\)90728-7](https://doi.org/10.1016/0024-3205(82)90728-7)
- 586 **Muthal, A. V., Mandhane, S. N. and Chopode, C. T.** (1997) Central administration  
587 of FMRFamide produces antipsychotic-like effects in rodents. *Neuropeptides* **31**,319-  
588 322. doi: [10.1016/s0143-4179\(97\)90065-2](https://doi.org/10.1016/s0143-4179(97)90065-2)
- 589 **Neher, E.** (1971). Two fast transient current components during voltage-clamp on  
590 snail neurons. *J. Gen. Physiol.* **58**, 36-53. doi: [10.1085/jgp.58.1.36](https://doi.org/10.1085/jgp.58.1.36)
- 591 **Nelson, L. S., Kim, K., Memmott, J. E. and Li, C.** (1998). FMRFamide-related gene  
592 family in the nematode, *Caenorhabditis elegans*. *Mol. Brain Res.* **58**, 102-111. doi:  
593 [10.1016/s0169-328x\(98\)00106-5](https://doi.org/10.1016/s0169-328x(98)00106-5)

- 594 **Nishimura, M., Ohtsuka, K., Takahashi, H. and Yoshimura, M.** (2000). Role of  
595 FMRFamide-activated brain sodium channel in salt-sensitive hypertension.  
596 *Hypertension* **35**, 443-450. doi.org/10.1161/01.HYP.35.1.443
- 597 **Nowycky, M., Fox, A. P. and Tsien, R. W.** (1985). Three types of neuronal calcium  
598 channel with different calcium agonist sensitivity. *Nature* **316**, 440-443. doi:  
599 [10.1038/316440a0](https://doi.org/10.1038/316440a0)
- 600 **Ödholm, M. P., Williamson, R. and Jones, M. B.** (2000). Ionic currents in cardiac  
601 myocytes of squid, *Alloteuthis subulata*. *J. Comp. Physiol. B* **170**:11-20.  
602 doi.org/10.1007/s003600050002
- 603 **O'Donohue, T. L., Bishop, J. F., Chronwall, B. M. Groome, J. and Watson, W. H.**  
604 (1984). III. Characterization and distribution of FMRF-amide immunoreactivity in the  
605 rat central nervous system. *Peptides* **5**, 563-568. doi: [10.1016/0196-9781\(84\)90087-1](https://doi.org/10.1016/0196-9781(84)90087-1)
- 606 **Price, D. A. and Greenberg, M. J.** (1977). Structure of a molluscan cardioexcitatory  
607 neuropeptide. *Science* **197**, 670-671. doi: [10.1126/science.877582](https://doi.org/10.1126/science.877582)
- 608 **Price, D. A. and Greenberg, M. J.** (1989). The hunting of the FaRPs: distribution of  
609 the FMRFamide-related peptides (FaRPs). *Biol. Bull.* **177**, 198-205. doi:  
610 [10.2307/1541933](https://doi.org/10.2307/1541933)
- 611 **Raffa, R. B., Heyman, J. and Porreca, F.** (1986). Intrathecal FMRFamide (Phe-  
612 Met-Arg-Phe-NH<sub>2</sub>) induces excessive grooming behavior in mice. *Neurosci. Lett.* **65**,  
613 94-98. doi: [10.1016/0304-3940\(86\)90126-6](https://doi.org/10.1016/0304-3940(86)90126-6)
- 614 **Raffa, R. B. and Stone, D. J.** (1996). Could dual G-protein coupling explain [D-Met  
615 (2)] FMRFamide's mixed action *in vivo*? *Peptides* **17**, 1261-1265.
- 616 **Rémy, C., Guy, J., Pelletier, G. and Boer, H. H.** (1988). Immunohistological  
617 demonstration of a substance related to neuropeptide Y and FMRFamide in the  
618 cephalic and thoracic nervous systems of locust *Locusta migratoria*. *Cell Tissue Res.*  
619 **254**, 189-195. doi [10.1007/BF00220033](https://doi.org/10.1007/BF00220033)
- 620 **Saidel, W. M.** (1979). Relationship between photoreceptor terminations and  
621 centrifugal neurons in the optic lobe of octopus, *Cell Tissue Res.* **204**, 463-472. doi:  
622 [10.1007/bf00233657](https://doi.org/10.1007/bf00233657)
- 623 **Saito, M. and Wu, C. F.** (1991). Expression of ion channels and mutational effects in  
624 giant drosophila neurons differentiated from cell division arrested embryonic



- 625 neuroblasts. *J. Neurosci.* **11(7)**, 2135-2150. doi: [10.1523/JNEUROSCI.11-07-](https://doi.org/10.1523/JNEUROSCI.11-07-02135.1991)  
626 [02135.1991](https://doi.org/10.1523/JNEUROSCI.11-07-02135.1991)
- 627 **Sasayama, Y., Katoh, A., Oguro, C., Kambegawa, A. and Yoshizawa, H.** (1991)  
628 Cells showing immunoreactivity for calcitonin or calcitonin gene-related peptide  
629 (CGRP) in the central nervous system of some invertebrates, *Gen. Comp. Endocrinol.*  
630 **83**, 406–414. doi: [10.1016/0016-6480\(91\)90146-w](https://doi.org/10.1016/0016-6480(91)90146-w)
- 631 **Schneider, L. E. and Taghert, P. H.** (1988). Isolation and characterization of a  
632 *Drosophila* gene that encodes multiple neuropeptide related to Phe-Met-Arg-Phe-NH<sub>2</sub>  
633 (FMRFamide). *Proc. Natl. Acad. Sci. USA* **85**, 1993-1997. doi:  
634 [10.1073/pnas.85.6.1993](https://doi.org/10.1073/pnas.85.6.1993)
- 635 **Scott, R. H., Pearson, H. A. and Dolphin, A. C.** (1991). Aspects of vertebrate  
636 neuronal voltage-activated calcium currents and their regulation. *Prog. Neurobiol.* **36**,  
637 485-520. doi: [10.1016/0301-0082\(91\)90014-r](https://doi.org/10.1016/0301-0082(91)90014-r)
- 638 **Sorenson, R. L., Sasek, C. A. and Elde, R.P.** (1984) Phe-Met-Arg-Phe-amide  
639 (FMRF-NH<sub>2</sub>) inhibits insulin and somatostatin secretion and anti-FMRFA-NH<sub>2</sub> sera  
640 detects pancreatic polypeptide cells in rat islet. *Peptides* **5**, 777-782.  
641 [https://doi.org/10.1016/0196-9781\(84\)90021-4](https://doi.org/10.1016/0196-9781(84)90021-4)
- 642 **Suzuki, H., Yamamoto, T., Inenaga, M. and Uemura, H.** (2000). Galanin-  
643 immunoreactive neuronal system and localization with serotonin in the optic lobe and  
644 peduncle complex of the octopus (*Octopus vulgaris*), *Brain Res.* **865**, 168–176. doi:  
645 [10.1016/s0006-8993\(00\)02191-0](https://doi.org/10.1016/s0006-8993(00)02191-0)
- 646 **Suzuki, H., Yamamoto, T., Nakagawa, M. and Uemura, H.** (2002). Neuropeptide  
647 Y-immunoreactive neuronal system and colocalization with FMRFamide in the optic  
648 lobe and peduncle complex of octopus (*Octopus vulgaris*). *Cell. Tissue Res.* **307**, 255-  
649 264. doi: [10.1007/s00441-001-0492-9](https://doi.org/10.1007/s00441-001-0492-9)
- 650 **Tasaki, I. and Hagiwara, S.** (1957). Demonstration of two stable potential states in  
651 the squid giant axon under tetraethylammonium chloride. *J. Gen. Physiol.* **40**, 859-  
652 885. doi: [10.1085/jgp.40.6.859](https://doi.org/10.1085/jgp.40.6.859)
- 653 **Tasaki, K., Tsukahara, Y., Suzuki, H. and Nakaye, T.** (1982). Two types of  
654 inhibition in the cephalopod retina. In Kaneko A, Tsukahara N, Uchizono K (eds)  
655 Neurotransmitters in the Retina and the Visual Centers. Biomedical Res. Suppl,  
656 Tokyo pp 41-44.



- 657 **Thiemermann, C., Al-Damluji, S., Hecker, M. and Vane, J. R.** (1991). FMRF-  
658 amide and L-Arg-l-Phe increase blood pressure and heart rate in the anaesthetized rat  
659 by central stimulation of the sympathetic nervous system. *Biochem. Biophys. Res.*  
660 *Commun.* **175**, 318-324. doi: [10.1016/s0006-291x\(05\)81237-9](https://doi.org/10.1016/s0006-291x(05)81237-9)
- 661 **Thompson, S. H.** (1977). Three pharmacologically distinct potassium channels in  
662 molluscan neurons. *J. Physiol. (Lond)* **265**, 465-488. doi:  
663 [10.1113/jphysiol.1977.sp011725](https://doi.org/10.1113/jphysiol.1977.sp011725)
- 664 **Walker, R. J., Papaioannou, S. and Holden-Dye, L.** (2009). A review of  
665 FMRFamide and RFamide-like peptides in metazoa. *Invertebr. Neurosci.* **9**, 111–153.  
666 doi: [10.1007/s10158-010-0097-7](https://doi.org/10.1007/s10158-010-0097-7)
- 667 **Wang, X., McKenzie, J. S. and Kemm, R. E.** (1996) Whole cell calcium currents in  
668 acutely isolated olfactory bulb output neurons of the rat. *J. Neurophysiol.* **75**, 1138-  
669 1151. doi: [10.1007/s10158-010-0097-7](https://doi.org/10.1007/s10158-010-0097-7)
- 670 **Wang, X. Y., Morishita, F., Matsushim, O. and Fujimoto, M.** (2000). Carassius  
671 RFamide, a novel FMRFa-related peptide, is produced within the retina and involved  
672 in retinal information processing in cyprinid fish. *Neurosci. Lett.* **289**, 115-118. doi:  
673 [10.1016/s0304-3940\(00\)01281-7](https://doi.org/10.1016/s0304-3940(00)01281-7)
- 674 **Williamson, R. and Chrachri, A.** (2004). Cephalopod Neural Networks  
675 *Neurosignals* **13**, 87-98. doi: [10.1159/000076160](https://doi.org/10.1159/000076160)
- 676 **Wu, J. and Lipsius, S. L.** (1990). Effects of extracellular Mg<sup>2+</sup> on T- and L-type Ca<sup>2+</sup>  
677 currents in single atrial myocytes. *Am. J. Physiol.* **259**, H1842-H1850.  
678 doi.org/[10.1152/ajpheart.1990.259.6.H1842](https://doi.org/10.1152/ajpheart.1990.259.6.H1842)
- 679 **Yakel, J. L.** (1991). The neuropeptide FMRFamide both inhibits and enhances the  
680 Ca<sup>2+</sup> current in dissociated *Helix* neurones via independent mechanisms. *J.*  
681 *Neurophysiol.* **65**, 1517-1527. doi.org/[10.1152/jn.1991.65.6.1517](https://doi.org/10.1152/jn.1991.65.6.1517)
- 682 **Yamamoto, T., Tasaki, K., Sugawara, Y. and Tonosaki, A.** (1965). Fine structure  
683 of octopus retina. *J. Cell. Biol.* **25**, 345-359. doi: [10.1083/jcb.25.2.345](https://doi.org/10.1083/jcb.25.2.345)
- 684 **Yamamoto, M. and Takasu, N.** (1984). Membrane-particles and gap-junctions in the  
685 retinas of 2 species of cephalopods, *Octopus ocellatus* and *Sepiolla japonica*. *Cell*  
686 *Tissue Res.* **237** (2), 209-218. doi: [10.1007/BF00217138](https://doi.org/10.1007/BF00217138)
- 687 **Young, J. Z.** (1962). The optic lobe of *Octopus vulgaris*, *Philos. Trans. R. Soc. B*  
688 *Biol. Sci.*, **245**, 19–58. doi.org/[10.1098/rstb.1962.0004](https://doi.org/10.1098/rstb.1962.0004)

- 689 **Young, J. Z.** (1971). The anatomy of the nervous system of *Octopus vulgaris*.  
690 Clarendon, Oxford. doi: [10.3389/fphys.2019.01637](https://doi.org/10.3389/fphys.2019.01637)
- 691 **Young, J. Z.** (1974). The central nervous system of *Loligo*. I. The optic lobe. *Phil.*  
692 *Trans. R. Soc. B Lond.* **267**, 263-302. doi.org/[10.1098/rstb.1974.0002](https://doi.org/10.1098/rstb.1974.0002)
- 693 **Zhu, Y., Sun, L.L., Wu, J.H., Liu, H., Zheng, L., Lü, Z. and Chi, C.** (2020). An  
694 FMRFamide Neuropeptide in Cuttlefish *Sepia pharaonis*: Identification,  
695 Characterization, and Potential Function. *Molecules* (Basel, Switzerland). Apr; 25(7).  
696 doi: [10.3390/molecules25071636](https://doi.org/10.3390/molecules25071636)
- 697

698 **Figure legends**

699 **Fig. 1 Morphology and overall ionic currents recorded from an identified**  
700 **centrifugal neuron in the optic lobe of cuttlefish. A)** Lucifer yellow-filled  
701 centrifugal neuron with the characteristic numerous fine branches in the plexiform  
702 zone (*arrow heads*). o.gr.: outer granule cell layer, pl: plexiform zone and i.gr.: inner  
703 granule cell layer. **B)** An evoked antidromic action current resulting from stimulation  
704 of the appropriate optic nerve bundle. **C)** Whole-cell currents recorded from a  
705 centrifugal neuron. Overall response to a series of voltage steps (with 20 mV  
706 increments) from a holding potential of -60 mV is composed of an outward current  
707 (*open circle*), a transient inward current (*filled circle*) and a smaller inward current  
708 (*filled triangle*). **D)** *I-V* plots of the outward current (*open circles*) and an inward  
709 current (*filled circles*). Horizontal bar: 50  $\mu\text{m}$  (**A**).

710

711 **Fig. 2 Voltage and pharmacological separation of A-current in an identified**  
712 **centrifugal neuron. A)** Whole cell outward current in response to membrane  
713 depolarization to voltage steps from a holding potential of -60 mV. Total outward  
714 current is composed of a transient outward current and a sustained outward current. **B)**  
715 Whole cell outward current in response to membrane depolarization to the same  
716 voltage steps as in **A** but this time from a holding potential of -40 mV. The A-current  
717 is largely inactivated at this holding potential, leaving only the sustained outward  
718 current or delayed rectifier ( $I_K$ ). **C)** Computer subtraction of **B** and **A** to show the  
719 isolated transient outward current or A-current ( $I_A$ ). **D)** *I-V* plots of the instantaneous  
720 currents 5 ms after the start of the voltage steps for the total outward current (*circles*),  
721 the mainly  $I_K$  current (*squares*) and the isolated  $I_A$  (*triangles*). **E)** Whole cell outward  
722 current in response to membrane depolarization to a voltage step of +50 mV from a  
723 holding potential of -80 mV. Total outward current is composed of a transient outward  
724 current and a sustained outward current (control). Bath application of 4 mM 4-AP  
725 suppressed the transient outward current, leaving only the sustained outward current  
726 (4-AP). Bath application of TEA suppressed 75% of this sustained outward current. **F)**  
727 *I-V* plots of the instantaneous currents 5 ms after the start of the voltage steps for the  
728 total outward current (*open circles*), the mainly  $I_K$  current (*filled circles*) and after the  
729 application of TEA (*filled triangles*).

730

731 **Fig. 3 Inward currents recorded from an identified centrifugal neuron. A)** In the  
732 control, the whole-cell currents from this cell obtained in response to a series of  
733 voltage steps (*bottom*), from a holding potential of -60 mV. **B)** 5 minutes after bath  
734 application of an ASW containing TTX (1 $\mu$ M), the Na<sup>+</sup> current disappeared leaving  
735 only a sustained inward current. **C)** TTX-sensitive current in isolation, which is  
736 obtained by computer subtraction of **B** from **A**.

737

738 **Fig. 4 Identification of the L-type calcium current. A)** Effect of barium chloride on  
739 the sustained inward current, whole cell inward current in a centrifugal neuron in  
740 response to a voltage step to 0 mV from a holding potential of -60 mV before  
741 (*control*) and after (*BaCl<sub>2</sub>*) substitution of barium for calcium in the external solution  
742 which resulted in an increase in the amplitude of the calcium current. **B)** Effect of  
743 cobalt chloride at a concentration of 4 mmol l<sup>-1</sup> on the sustained inward current, whole  
744 cell inward current in a centrifugal neuron in response to a voltage step to -10 mV  
745 from a holding potential of -60 mV before (*control*) and after (*CoCl<sub>2</sub>*) was added into  
746 the external solution resulted in total blockade of the calcium current. **C)** Similarly,  
747 nifedipine (5  $\mu$ mol l<sup>-1</sup>) also suppressed completely this sustained calcium current. **D)**  
748 Representative example of membrane currents during a test-pulse to -30 mV from a  
749 holding voltage of -80 mV (a) or -60 mV (b); the difference current (a-b) is the T-type  
750 Ca<sup>2+</sup> current. **E)** Peak current-voltage (I/V) relation of the same centrifugal neuron.  
751 For this I/V plot current traces are displayed, when the holding potential was -80 mV  
752 (*open circles*), when the holding potential was -60 mV (*filled circles*), and finally the  
753 difference current (*triangles*).

754

755 **Fig. 5 FMRamide inhibits both the I<sub>A</sub> and I<sub>K</sub> in centrifugal neuron. A)** Current  
756 traces recorded in response to membrane depolarization to a voltage step of -60, -20,  
757 +20, +50, +60 and +70 mV from a holding potential of -60 mV prior to the  
758 application of FMRFa. **B)** Reduction of K<sup>+</sup> currents by FMRFa (1  $\mu$ M). **C)** Recovery  
759 of K<sup>+</sup> currents after FMRFa had been washed out. **D)** Difference current obtained by  
760 subtracting current profiles obtained in the presence of FMRFa (**B**) from those  
761 obtained before the application of FMRFa (**A**) demonstrates that FMRFa blocked both

762 the fast transient component,  $I_A$  (*arrow head*), as well as the sustained and slowly  
763 inactivating potassium current,  $I_K$  (*doubled arrow head*).

764

765 **Fig. 6 FMRFamide-mediated inhibition of  $I_{Na}$  and  $I_{Ca,L}$  in a centrifugal neuron.**

766 **A)** Current traces recorded in response to membrane depolarization to a voltage step  
767 of -10 mV from a holding potential of -60 mV before (*control*) and after (*FMRFa*)  
768 bath application of 1  $\mu$ M FMRFa, first after 5 minutes (*grey trace*) and then 8 minutes  
769 (*dark trace*). These currents trace not only show that FMRFa inhibited  $I_{Na}$  (*star*), but  
770 also  $I_{Ca,L}$  (*triangle*). **B)** I-V relationship of  $I_{Na}$  before (*open circles*), 5 minutes and then  
771 8 minutes after (*grey and filled circles*, respectively).

772

773 **Fig. 7 Effect of FMRFamide on calcium currents in centrifugal neuron. A)** Left

774 traces are current traces recorded in response to membrane depolarization to a voltage  
775 step of -40 mV from a holding potential of -80 mV showing that FMRFa had no  
776 apparent effect on the transient component of the calcium current. Right traces are  
777 current recorded in response to membrane depolarization of the same centrifugal  
778 neuron to a voltage step of 0 mV from a holding potential of -80 mV before (*black*  
779 *trace*) and after (*grey trace*) the application of FMRFa demonstrating that this  
780 neuropeptide decrease the amplitude of the  $I_{Ca,L}$ . **B)** I-V relationship of both calcium  
781 current under control conditions (*black circles*), and after the application of FMRFa  
782 (*grey circles*). **C)** Time course of the onset, and recovery from, the effect of  
783 FMRFamide on  $I_{Ca,L}$ .

784

785

786

787

788

Figures

Fig. 1

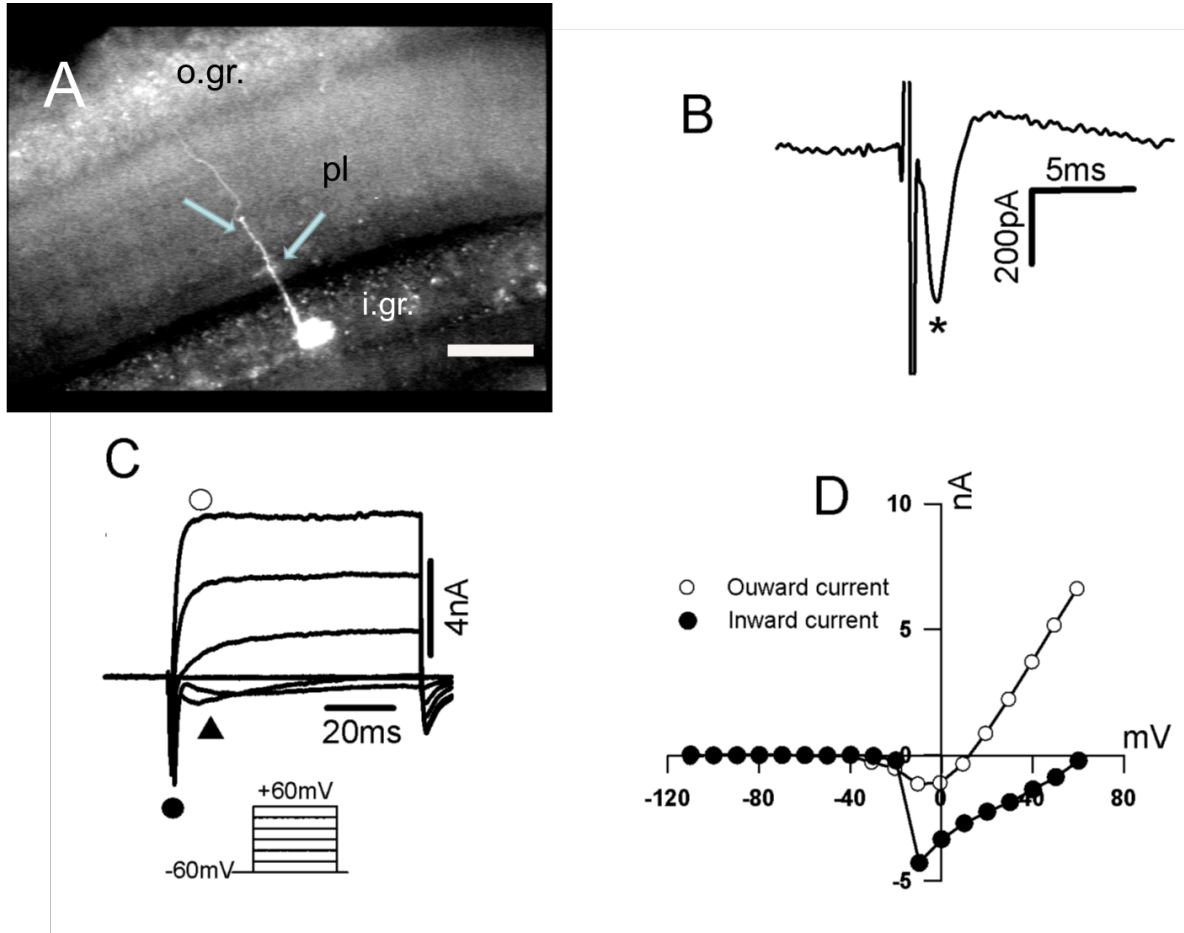


Fig.2

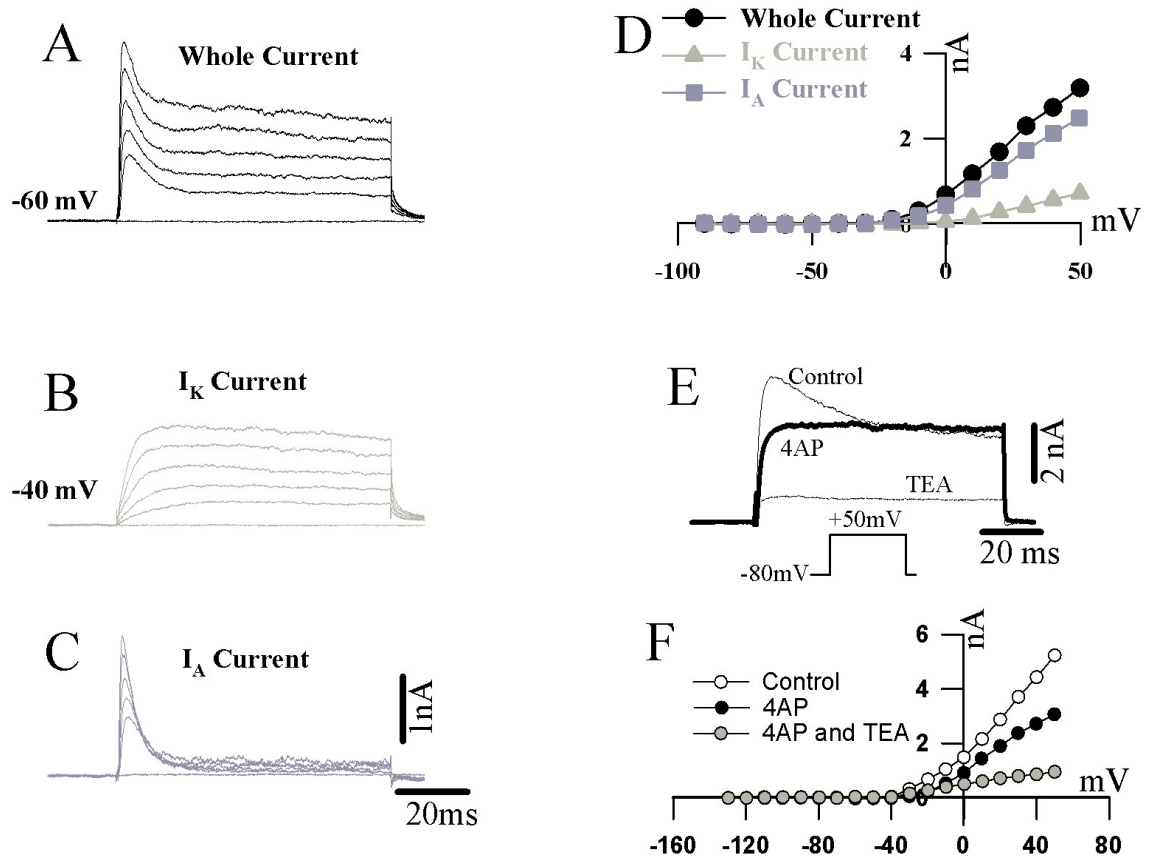


Fig.3

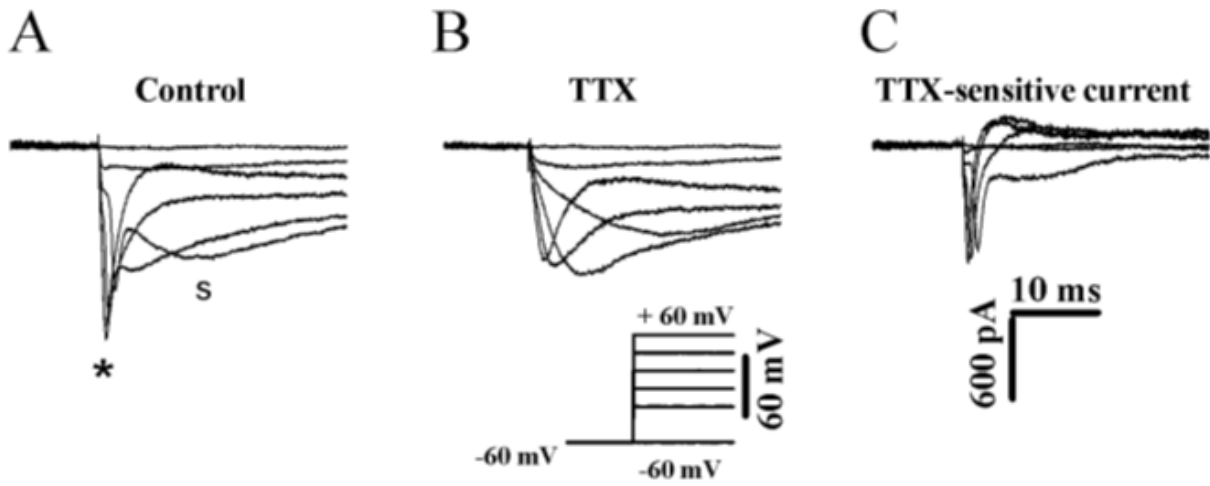


Fig.4

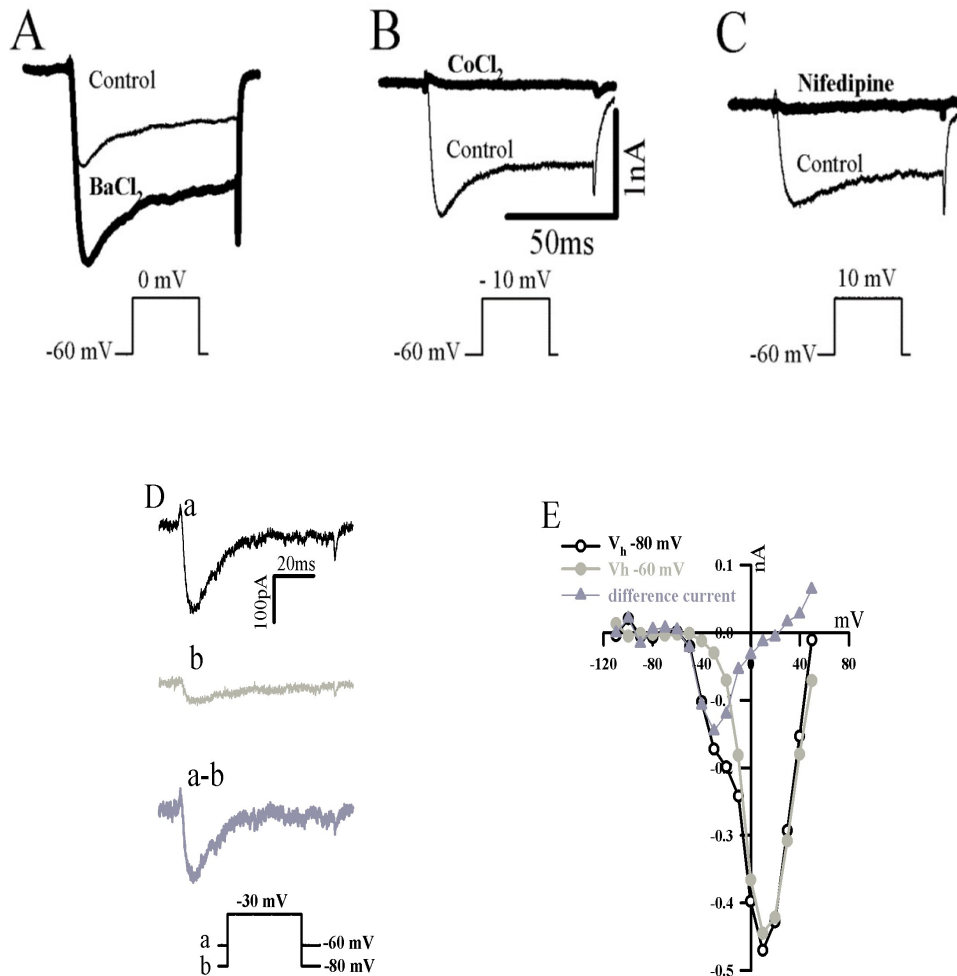




Fig.5

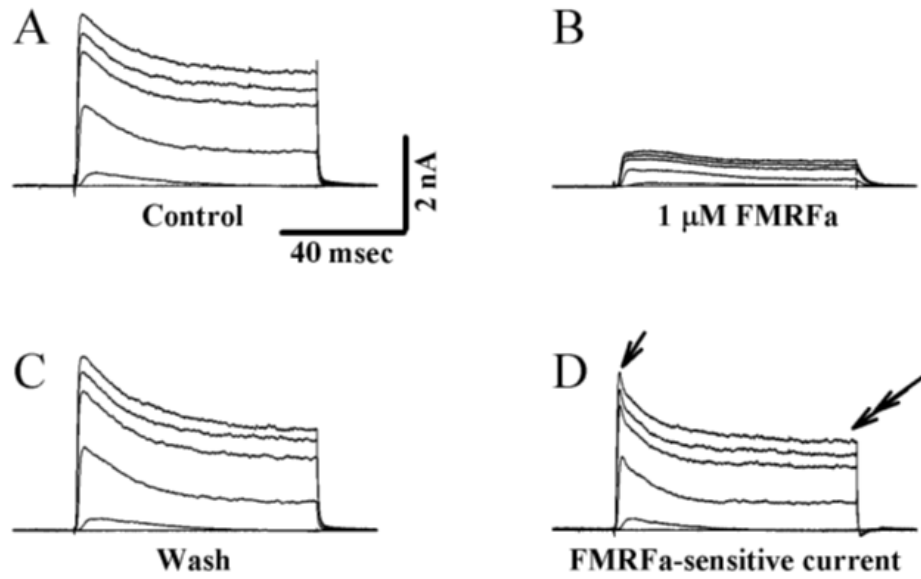


Fig.6

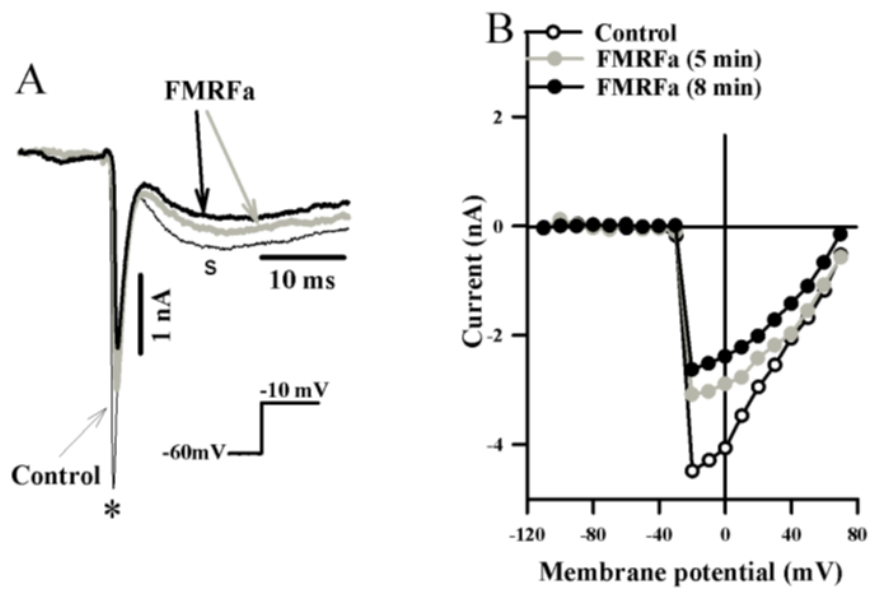


Fig.7

